Surface Science 650 (2016) 76–82

Contents lists available at ScienceDirect

Surface Science

journal homepage: www.elsevier.com/locate/susc

Noncontact atomic force and Kelvin probe force microscopy on MgO(100) and MgO(100)-supported Ba

Chi Lun Pang [a,b,*], Akira Sasahara [a,c,1], Hiroshi Onishi [b]

[a] Department of Chemistry, Faculty of Science, Kobe University, Kobe 657-8501, Japan
[b] Department of Chemistry and London Centre for Nanotechnology, London WC1H 0AJ, UK
[c] CREST, Japan Science and Technology Agency, Kawaguchi, Saitama 332-0012, Japan

ARTICLE INFO

Available online 9 October 2015

Keywords:
Noncontact atomic force microscopy
Kelvin probe force microscopy
MgO(100)
Barium
Hydroxyl
NO_x

ABSTRACT

Atomically-flat MgO(100) surfaces were prepared by sputtering and annealing. Noncontact atomic force microscopy (NC-AFM) and Kelvin probe force microscopy (KPFM) were used to characterize the MgO(100) surfaces. The NC-AFM images revealed the presence of point defects on an atomically-resolved surface. The surface potential at these point defects, as well as features such as step edges and deposited Ba nanoparticles were mapped using KPFM. The Kelvin images show that the surface potential increases at the point defects and at the step edges. On the other hand, a decrease in the potential was found over Ba nanoparticles which can be explained by electron charge transfer from the Ba to the MgO.

1. Introduction

Metal and metal oxide nanoparticles supported on metal oxide surfaces are a very important class of material that are employed, for example, in catalysis and in electronics [1,2]. This has led to extensive study of their surface science. MgO(100) has long been employed as a model oxide surface due partly to the ease of sample preparation through cleaving [3]. More recently, alkaline earth oxides, especially BaO, have also received considerable attention because of their activity in NO_x storage [4–6]. For instance, alumina-supported BaO nanoparticles are employed in automobile catalysts [5].

Charge transfer between nanoparticles and their supports is thought to be important in catalysis [1,7]. Such charge transfer processes can be directly followed particle-by-particle using Kelvin probe force microscopy (KPFM) whereby the surface potential is measured simultaneously with non-contact atomic force microscopy (NC-AFM) [8–19].

It has proven difficult to image insulating oxides using NC-AFM and although several studies resolve steps or supported nanoparticles [20–31], only a few reach atomic resolution [21,23,27,29,31–35]. The difficulty in imaging these insulating oxides is probably related to strong surface charging [28,30]. Given that the technique is a modification of NC-AFM, it follows that there are only a handful of KPFM studies on insulating oxides [12,15–17].

In this article, we present NC-AFM and KPFM studies of MgO(100) and MgO(100)-supported Ba nanoparticles. Previously, MgO(100) surfaces have been formed by cleaving [3,12,16,25,28–30,35,36], annealing in air [37], preparation of thin films [17,38–41] or by the use of smokes and nanocubes [42,43], as well as by sputtering and annealing in UHV to 1600 K [20]. Here, we prepare our MgO(100) surfaces by sputtering and annealing to a higher temperature of ~1700 K. Our preparation led to large, flat terraces, generally 100–1000 Å in width, that could be imaged with atomic resolution in NC-AFM, including the resolution of individual point defects. KPFM images reveal an increase in the surface potential at the point defects and at the step edges whereas a decrease in the potential was found over Ba nanoparticles which can be explained by electron charge transfer from the Ba to the MgO.

2. Experimental details

The experiments were performed using a JSPM-4500A (JEOL) microscope operated at room temperature and housed in an ultra-high vacuum (UHV) chamber with a base pressure of ~2×10^{-10} mbar. NC-AFM images were recorded using conductive silicon cantilevers (MikroMasch) with resonant frequencies (f_0) of 280–365 kHz and force constants of ~14 Nm^{-1}. Peak-to-peak amplitudes (A_{p-p}) ranged from 70–135 Å. After approaching the tip to the sample, the apparent local contact potential difference (LCPD) between the two was found from a plot of the frequency shift (Δf) vs. applied bias [12,28], and a static compensating bias (V_{bias}) was applied to the sample during NC-AFM measurements.

KPFM measurements were conducted in the frequency modulation mode where an AC voltage, with a peak-to-peak amplitude (A_{p-p}) of 2 V and a frequency of 2 kHz, as well as a DC bias voltage (V_{CPD}) were

* Corresponding author at: Department of Chemistry and London Centre for Nanotechnology, London WC1H 0AJ, UK. Tel.: +44 207 679 5580; fax: +44 207 679 0595.
E-mail address: chi.pang@ucl.ac.uk (C.L. Pang).
[1] Present address: Japan Advanced Institute of Science and Technology, Nomi, Ishikawa 923-1292, Japan.

http://dx.doi.org/10.1016/j.susc.2015.09.022
0039-6028/

additionally applied to the tip. The DC bias is the voltage applied to compensate the local contact potential difference (LCPD) at each point of the image. All KPFM images were recorded in the constant frequency shift (Δf) mode with a scanning speed of 1.7 s/line. On an insulator, charged defects both at the surface or in the bulk can be detected as a modification of the LCPD [12,15,16,19,44].

The MgO(100) crystals (Shinkosha) were 7 mm × 1 mm × 0.3 mm in size and prepared with cycles of Ar-ion bombardment (2 keV) and annealing to ~1700 K by passing a current through a thin piece of Ta foil pressed against the back of the sample. Ba was vapour-deposited from a getter source (SAES) onto the as-prepared MgO(100) sample that was held at ~800–900 K in order to grow large clusters clearly attributable to Ba. Following evaporation, the sample was annealed for ~1 min at 1300 K to further increase the Ba particle size.

3. Results and discussions

Fig. 1a shows an NC-AFM image of the MgO(100) surface after several cleaning cycles. The height between terraces is ~2 Å, consistent with the minimum expected step height for MgO(100). Small bright features can be seen both on the terraces and decorating the step edges and some of these are circled in the figure.

Fig. 1b shows a higher resolution NC-AFM image of the surface. Here, the features on the terraces have resolved into small protrusions with a density of ~0.01 monolayers (ML) where 1 ML is defined as the density of primitive surface unit cells. The widths (FWHM) of these protrusions is ~5 Å which is consistent with the size expected from individual point defects. There are several candidates for point defects on MgO(100), including O or Mg vacancies (vacs), ad-O atoms, ad-Mg atoms, segregated calcium and carbon, as well as adsorbates from the residual vacuum [20,45–49].

There are 88 bright point defects in Fig. 1b and of these, 70 appear to be paired with only 18 isolated defects. The closest separation of these pairs is ~6 Å in the <110> directions. Such a separation is too long to originate from a direct bond. One possible explanation for the pairing is that it results from water dissociation in surface O-vacs, the source of water being the residual vacuum. In such a scenario, the water would split with the –OH fragment filling the O-vac and the –H fragment adsorbing on a nearby O ion. Thus, two H adatoms would be formed from each water molecule and given the relatively high barrier to diffusion for the H adatoms (~1.2 eV) [50] we would expect to observe pairs of OH groups. Pairs of OH groups have been observed on TiO_2(110) [51–55] but this is largely due to the high barrier calculated for the first hop (1.22 eV) [52]. STM measurements of subsequent hopping indicate a much lower barrier of ~0.8 eV [52]. Sequential images (e.g. that in Fig. 1b,c) confirm that the point defects are immobile at least on the timescale of several minutes. Dissociation of other common impurities in the residual vacuum such as CO and CO_2 would not give rise to two equivalent fragments. While this explanation of the paired defects being hydroxyl is feasible, a more definitive assignment would require further study. For example, the proposed dissociation of water at the vacancies could be directly visualized with atomically-resolved imaging before and after active dosing of water. This pairing is not apparent in Fig. 1a because of the lower resolution of the image.

Fig. 2 shows two sequential images taken from the same surface as those in Fig. 1. Between the two images, there is an adventitious tip change that leads to an inversion in the contrast of the point defects from bright to dark. Similar contrast inversions have been explained by a change in the nature of the tip apex [36,54–58], the most simple of which involves a change in the potential. If the tip apex has a negative potential, it will be attracted for example to a positive H adatom which will therefore appear bright in the NC-AFM images. On the other hand, changing the polarity at the tip apex to a positive potential means the tip apex will be repelled by the H adatom so that it will appear dark in the NC-AFM images instead.

Previous sample preparations of MgO(100) by sputtering/annealing did not lead to atomically-resolved images, presumably because the annealing temperature (1600 K) was not sufficient to form a well-ordered atomically flat surface [20]. We found that samples annealed only to 1300 K were rough and contained large particles over 100 Å in height. On the other hand, after sputter/annealing cycles to ~1700 K, several different MgO(100) samples were imaged with atomic resolution images. Fig. 3 shows one such example. The separation between the bright spots in the <001> directions is ~4 Å, consistent with NC-AFM images from UHV-cleaved and thin film MgO(100) [29,39], as well as STM images of the film [38,40,41]. A line profile in Fig. 3b highlights the atomic corrugation in the image. This periodicity is twice the separation between Mg and O ions along <001> (i.e. 2.1 Å), suggesting that only one sub-lattice, the Mg or the O sub-lattice, is imaged bright. However, we cannot identify which sub-lattice appears bright from our NC-AFM images alone. Definitive identification of similar sub-lattices in ionic surfaces is difficult in NC-AFM and usually only possible by using molecular markers, by careful comparison between experimental and theoretical simulations of NC-AFM images, analysis of force spectra, or a combination of the three [36,54–58]. As in Figs. 1 and 2, there are also several point defects present that appear as small protrusions (one of which is circled). The point defects have a coverage of ~0.04 ML and have a streaky appearance. While such streakiness is

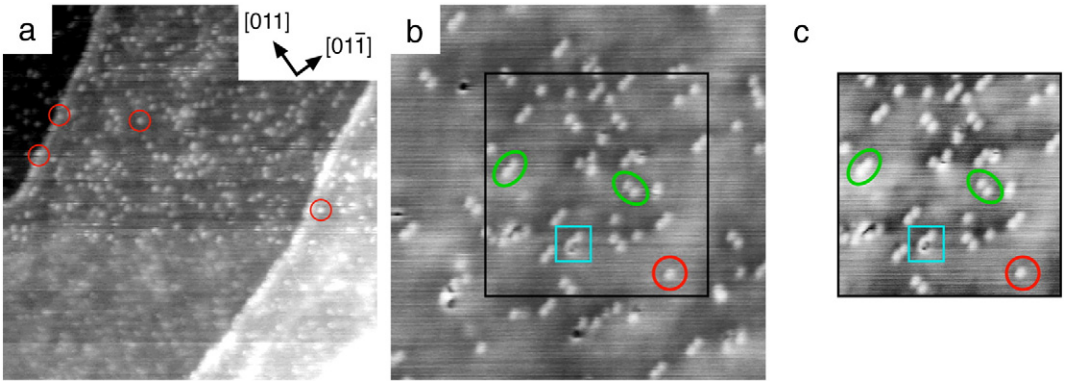

Fig. 1. NC-AFM images of the same sputtered and annealed MgO(100) surface recorded with $f_0 \cong 340$ kHz. (a) (1000 Å)^2 image with $\Delta f = -17$ Hz, $A_{p-p} \cong 70$ Å, and $V_{bias} = -2.0$ V. Some bright features at the steps and terraces are circled red. (b) (250 Å)^2 image with $\Delta f = -58$ Hz, $A_{p-p} \cong 70$ Å, $V_{bias} = -6.0$ V. Examples of paired and single bright defects are circled green and red, respectively. The black square indicates where the image in (c) was taken from. (c) (150 Å)^2 image with $\Delta f = -61$ Hz, $A_{p-p} \cong 70$ Å, $V_{bias} = -6.0$ V. The markers are the same as in (b). Note that in (b) and (c), there is a slight elongation of the defects in the [01$\bar{1}$] direction due to the tip shape. In (b) and (c), a small number of dark regions are also present, one of which is highlighted with a light-blue square. These dark regions have rather abrupt changes in the contrast and we attribute this to some imaging artefact perhaps due to the slow response of feedback loop.